



Prediction of Low-velocity Impact Damage in Sandwich Composite Beams

Solver I. Thorsson* , Jiawen Xie* , Jaspar Marek † and Anthony M. Waas ‡

University of Michigan, Ann Arbor, MI, 48109-2140

A characteristic failure mechanisms that is observed in the damage evolution of laminated composite beams subjected to low velocity impact is delamination interacting with matrix cracking. This failure mode can be studied in isolation by investigating the low velocity impact response of sandwich panels where thin face sheets are bonded to a core. In these panels, failure is seen to initiate in the core by cracking, leading to delamination between the core and the face sheet. Results for the flexural response and failure mechanisms of sandwich composite beams under three point bend loading, both for quasi-static and dynamic loading are presented. Digital image correlation (DIC) technique is used to obtain the surface strain field during the response event as well as capturing the onset of failure. A 2D, plane strain finite element (FE) model using the Smeared Crack Approach (SCA) has been developed to predict the response and interactive failure seen in the experiments. The FE model accurately captures the response seen in the experiments as well as the mode of failure and the progression.

I. Introduction

Engineers need a better understanding of the damage observed in composites subject to impact. However, modeling the impact dynamic response in composites, using finite element based approaches can be computationally expensive due to complex failure mechanisms and interactions amongst them during the damage and failure event. Previous studies have found comparable load-displacement responses, and similar damage distributions and force levels between quasi-static and low-velocity impact tests.^{1,2} The failure observed in multi-ply cross ply composite laminates subject to low velocity impact has been reported³ and it is observed that a characteristic failure mechanism is the interaction between transverse matrix cracking and delamination. Thus, it is of interest to study this failure mode in isolation. Because of the similarity between failure mechanisms in a multi-layered composite laminate and those that occur in a sandwich panel, under flexural response, it is expedient to investigate failure mode interaction and progression in a sandwich panel, where the flexural rigidity of the specimen can be tailored to experimental requirements. The impact response of sandwich panels display transverse shear failure and delamination which is similar to failure observed in multi-layered laminates subjected to similar loading conditions.

In this paper we will present both experimental results and computational results on the flexural response and failure of sandwich composite beams under quasi-static and dynamic three point bend loading. The motivation for this study is to clearly understand the interaction between different failure mechanisms, in this case the shear failure of the core and the delamination of the interface. Sandwich composites with two significantly different materials with respect to mechanical behavior (face sheet and core) can be expected to have a relatively neat failure mechanism. This study could therefore prove very useful for developing modeling strategies to understand failure in laminated composites subject to low-velocity impact since laminated composites that often contain stacking sequences of (0/90/0) show transverse cracking in the 90 layers which

Copyright© 2015 by Solver I. Thorsson, Jiawen Xie, Jaspar Marek and Anthony M. Waas. Published with permission by the American Institute of Aeronautics and Astronautics.

*Graduate Student Research Assistant, Department of Aerospace Engineering.

†Visiting Research Assistant, Department of Aerospace Engineering.

‡Felix Pawlowski Collegiate Professor, Department of Aerospace Engineering, AIAA Fellow. From January 1, 2015, Boeing Egtvedt Chair and Chairman, Dept. of Aeronautics and Astronautics, University of Washington, Seattle.

lead to delaminations at the adjacent interfaces, a mechanism that is comparable to the failure initiating in the core of a sandwich structure leading to delamination at the face sheet-core interface.

II. Experimental Results

Three point bend tests were performed on a sandwich composite beam both statically and dynamically, the dimensions of the specimen (Table 1) and test fixture (Figure 1) were held constant for both events. The sandwich composite beam that was studied in this research has face sheets composed of 8 plies of T300B-3K plain woven carbon fiber laminae with a stacking sequence $(-45/45)_4$, and the face sheets are impregnated with Epon 862 epoxy. The core material used is LAST-A-FOAM-FR-6710, which is a brittle foam. The core thickness was chosen to be 12.7 mm thick.

Rubber pads were used between the rollers and the specimen to prevent stress localization which would result in indentation and crushing of the core under the roller (these results were found in preliminary testing that was done). The material used for the rubber pads was ultra-strength neoprene rubber with durometer 60A. During loading the rubber pads can be seen deforming excessively, making it seem as if the core is getting crushed underneath the roller, however with close observation it was concluded that the core is not getting crushed, the rubber pads are deforming out-of-plane and creeping over the face sheets. The static tests were performed on an MTS loading machine with a loading rate of 0.01 mm/second, this provides quasi-static loading conditions. The event was recorded at 1 frame every 5 seconds with a Nikon D5300 digital camera equipped with a 105 mm lens. The dynamic testing was conducted in a drop tower with an impact mass of 25.13 kg, different energy levels of impact were studied to establish the impact energy needed to fail the sandwich structure. The impact energy of interest proved to be 10 joules, the energy level gives repeatable failure in the structure as well as being close to the minimum required energy to produce failure. The impact event was captured using a Photron SA-2 high-speed camera recording at a rate of 25,000 frames per second with a resolution of 1024 pixels by 248 pixels.

Digital Image Correlation (DIC) techniques were used to obtain full field surface displacement and strain

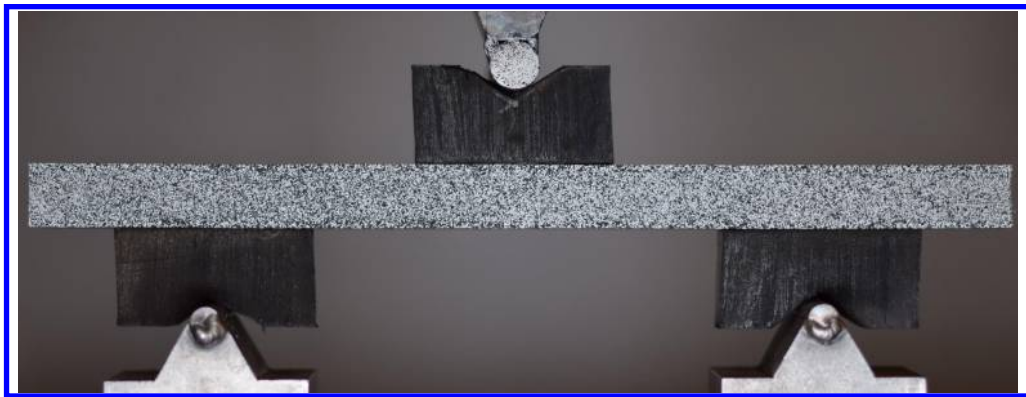


Figure 1. Three-point bend fixture.

Table 1. Key dimensions in experiments.

Beam length	250 mm
Span length	152.4 mm
Beam width	24 mm
Face-sheet thickness	1.9 mm
Core thickness	12.7 mm
Top roller diameter	12.7 mm
Bottom roller diameter	7.9 mm

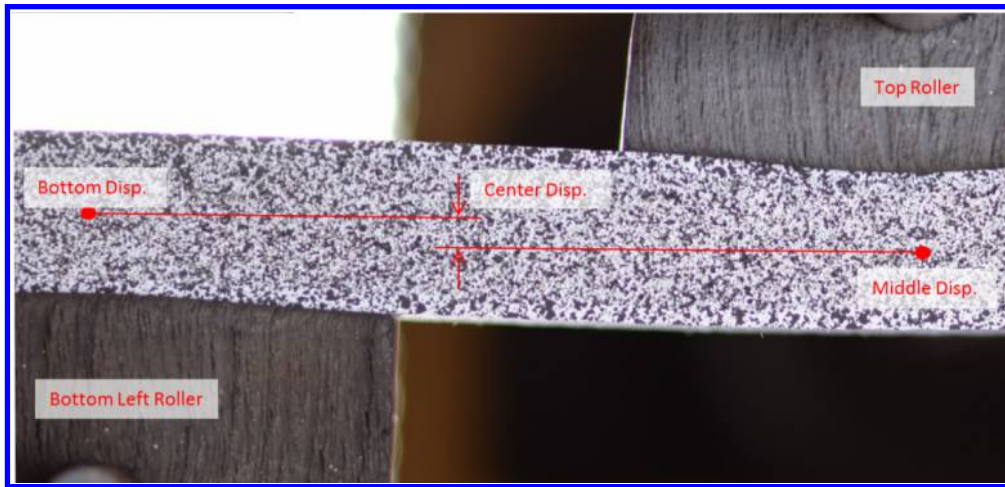


Figure 2. The definition of center displacement.

fields during the loading event. Due to the large deflection of the rubber pads, the displacement was collected digitally from the DIC data, where the vertical displacement is calculated from the difference between the displacement at the bottom rollers and at the top roller. This is done at the centerline of the sandwich beam, a schematic is shown in Figure 2.

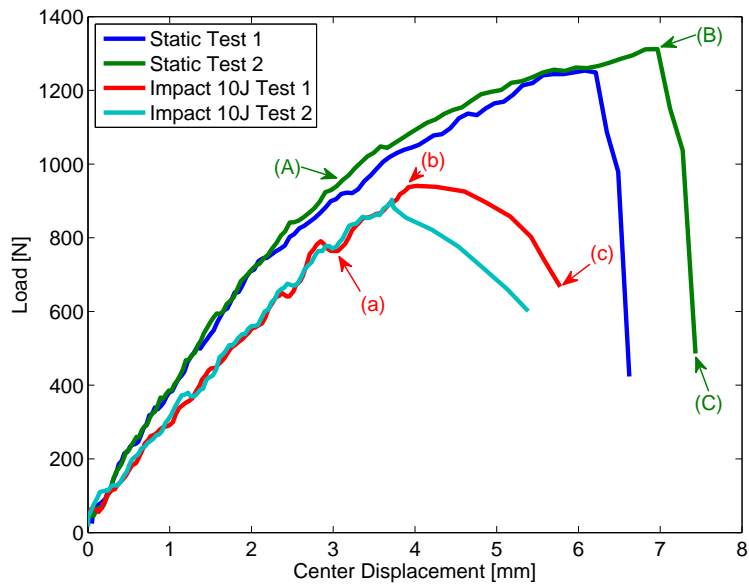
Multiple tests were done to make sure repeatability was established. Typical experimental load-displacement response plots can be seen in Figure 3(a), for quasi-static and dynamic loading, respectively. It can be seen from the static load-displacement response that after an initial fairly linear response, nonlinearity sets in due to the non-linear stress-strain response of the core material.⁴ This non-linear behavior is not present in the impact response of the sandwich beam, because the center displacement of the impact case is smaller than the corresponding quasi-static case, resulting in core shear strains that are smaller. The peak load for the impacted structure is also lower than for the quasi-statically loaded specimen as well as the stiffness being lower. The failure modes for the quasi-static and dynamic cases are in good agreement with each other, both of the tests show a highly catastrophic failure. With the use of the high-speed cameras the failure event can be seen more clearly. The structure can be seen going from no failure to complete failure in under 0.2 milliseconds, during which 5 frames showing the initiation and propagation, see Figure 4 of the failure event is captured. The initial failure is due to high shear stress in the core, and the location of shear failure showed consistency between tests. Figure 3(b) shows the strain progression as well as the onset of failure captured in the dynamic case. The quasi-static failure progression was not captured with the rate at which the cameras were recording. From the high-speed cameras the failure can be seen to initiate in the core close to the lower face sheet and then a crack propagates through the core at an angle of 45° . Once the crack reaches the face sheets, initially the lower one, it starts a delamination that grows very rapidly along the face-sheet-core interface. The delamination crack that formed at the bottom interface propagates all the way through to the edge while the delamination at the top interface arrests slightly to the side of the roller, opposite to the side where the core has cracked.

III. Finite Element (FE)-based Simulation

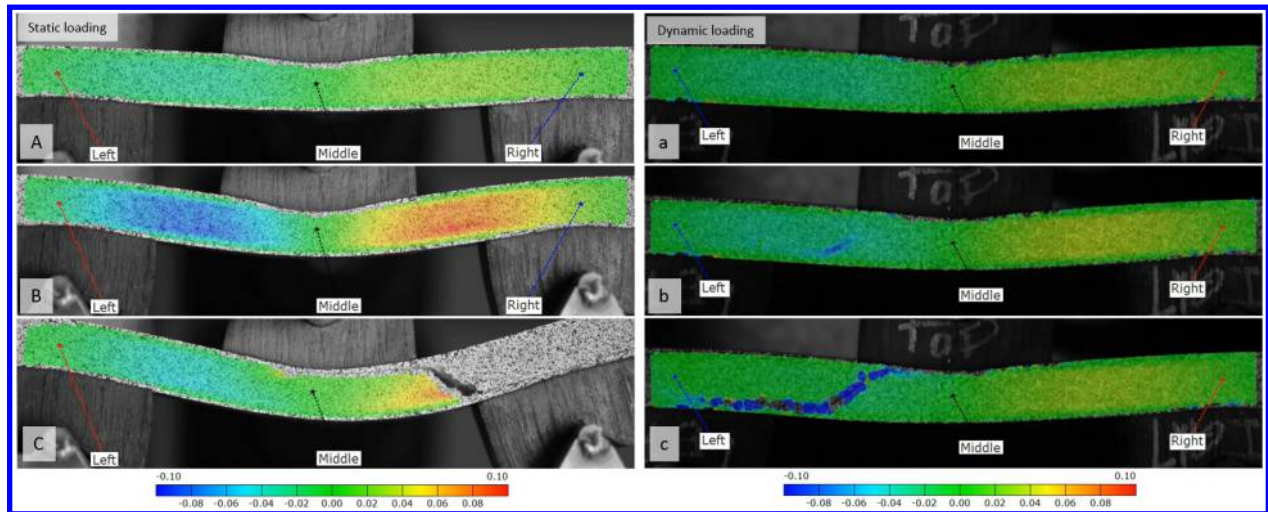
A. Modeling Details

The 2D configuration of the tests was built by using the commercial software package ABAQUS/Explicit, shown in Figure 5. The steel rollers, rubber pads and sandwich beam were modeled by four-noded plane-strain continuum elements with reduced integration (CPE4R). A friction coefficient of 0.5 was assigned to all contacts.

The element size of the core and face-sheets are $0.5 \text{ mm} \times 0.3 \text{ mm}$ and $0.5 \text{ mm} \times 0.2 \text{ mm}$ respectively. The face-sheet and the foam core mechanical properties are shown in Tables 2 and 3 respectively. The shear non-linearity is shown in Figure 6, and in this study only the foam core had a failure criterion defined. The evolution of core failure was modeled by using the Smeared Crack Approach (SCA), which has been



(a) Load-displacement response of quasi-static three-point bend and 10J impact tests



(b) DIC results of transverse shear strain: quasi-static three-point bend test (left) and 10J impact test (right)

Figure 3. Representative experimental results.

adapted from the study by Heinrich and Waas,⁵ who extended the original formulation of Rots et al.⁶ The 2D formulation of the SCA for an isotropic material as presented in⁷ and implemented through the user subroutine VUMAT, was used in the present study. An exponential traction separation law for the smeared crack strain has been adopted. The failure criterion used is the maximum tensile principle stress, of which the critical value is denoted as X_T . In experiments, the crack randomly occurs on either side of the top roller, and the failure initiation is caused by slight asymmetry in the strength properties of the core which are not homogeneous. Therefore, we introduced a *imperfect* model for the foam core, where the right half is 1.1 times stronger than the left half, in terms of critical tensile principle stress. Due to this choice, the core shear crack will always initiate in the left half, a slightly higher critical value will not significantly influence the crack propagation once the crack reaches the right half.

The density of the rubber pads is 1100 kg/m^3 . To achieve a better understanding of the mechanical properties of rubber pad material, uniaxial compression tests were performed on a wide rubber specimen. The dimension of the rubber specimen is $25.94 \text{ mm (L)} \times 136.15 \text{ mm (W)} \times 23.90 \text{ mm (H)}$. The rubber was

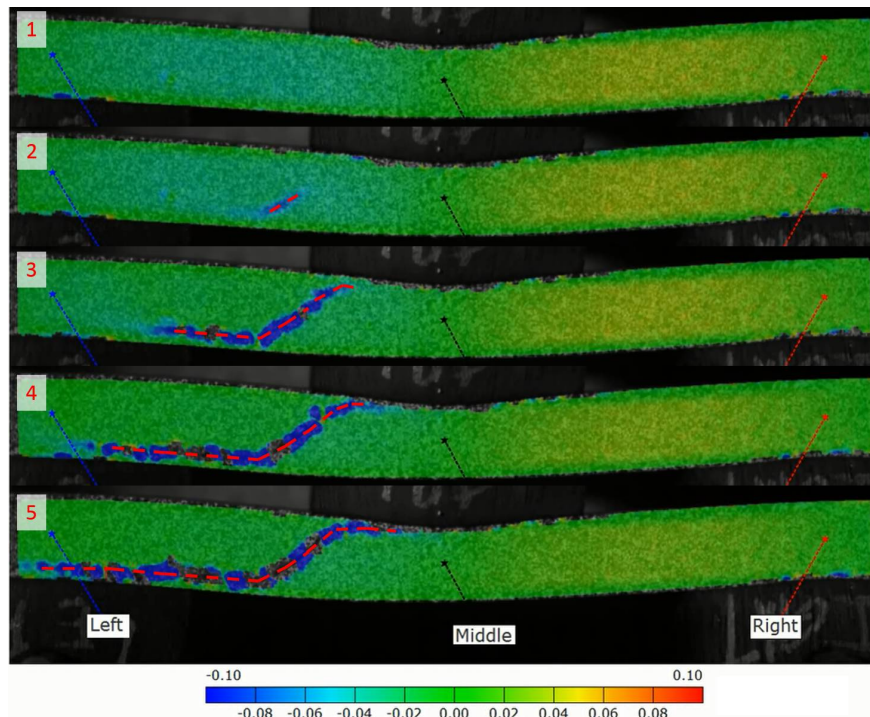


Figure 4. The failure event for the 10J impact. The interval between each picture is 0.04 milliseconds where the first image shows no damage. The dashed red line represents cracks.

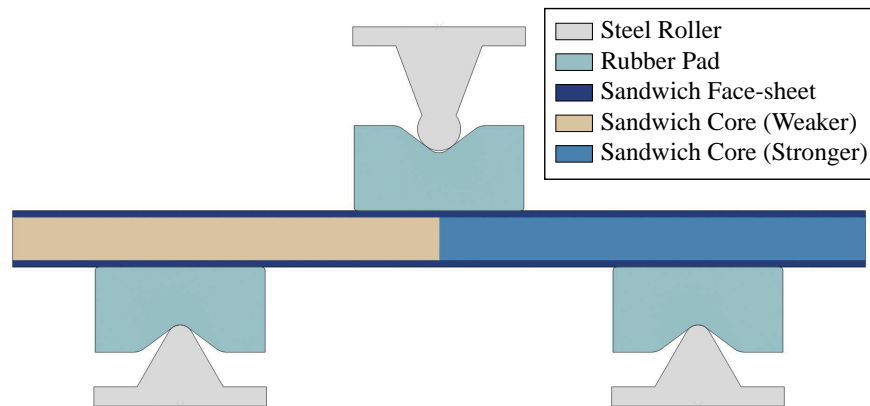


Figure 5. 2D plane-strain FE model of the sandwich composite with *imperfect* core

loaded in the thickness direction (H). The rubber specimen is wide enough so that it can be considered to satisfy plane-strain conditions. A 2D FE simulation was adopted to simulate the compression test. The cross-section of the rubber specimen was modeled by using continuum plane-strain elements (CPE4). Marlow's hyper-elastic model was used.⁸ The Poisson's ratio of the rubber was set as 0.495. As shown in Figure 7, the 2D FE model gives good agreement with the experimental results.

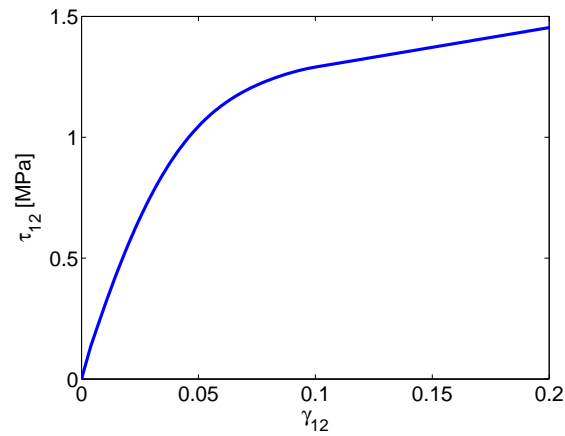
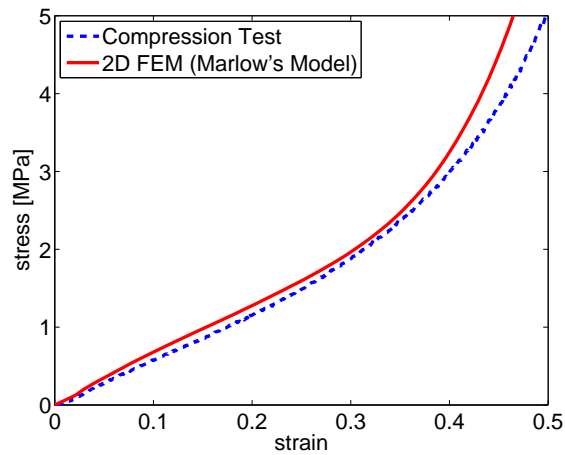
The steel rollers were modeled as rigid bodies. The impactor mass, 25.13 kg, was assigned as a point mass to the reference point of the top center roller. The quasi-static loading was simulated as a displacement controlled loading at the top center roller with loading rate 25 mm/s. The loading rate was chosen by considering the balance of precision and computational cost. Impact energy was applied to the model by specifying an initial velocity of the top center roller. The initial velocity for the 10J impact is 0.89 m/s.

Table 2. Mechanical properties of the face-sheets.

Density, ρ	1450 kg/m ³
Young's modulus, E	48.1 GPa
Poisson's ratio, ν	0.21

Table 3. Mechanical properties of the foam core.

Density, ρ	160 kg/m ³
Young's modulus, E	86 MPa
Poisson's ratio, ν	0.3
Tensile strength, X_T (static)	1.32 MPa
Tensile strength, X_T (dynamic)	1.1 MPa
Mode I energy release rate, G_{Ic}	0.05 N/mm

**Figure 6. Nonlinear shear stress-strain relation for the sandwich core material.****Figure 7. The stress-strain curve from a compression test on a long rubber specimen and FEM simulation of the test using CPE4 element and Marlow's hyperelastic model.**

B. Results

The computed load-displacement responses from the quasi-static simulations are compared against experimental results, as shown in Figure 8. Two different displacements are reported. Figure 8(a) uses the roller

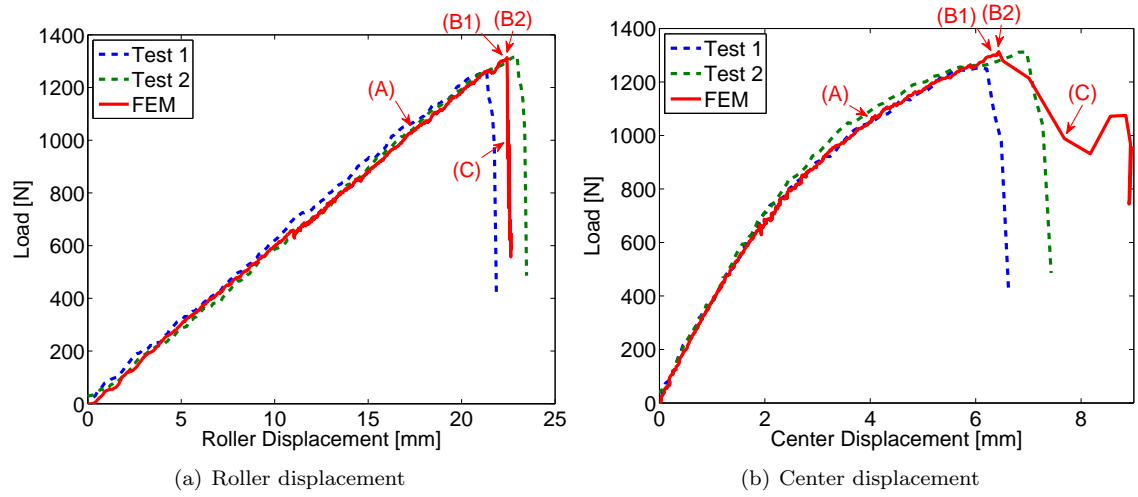


Figure 8. Comparisons of load-displacement response between experiments and FEM simulation of quasi-static test.

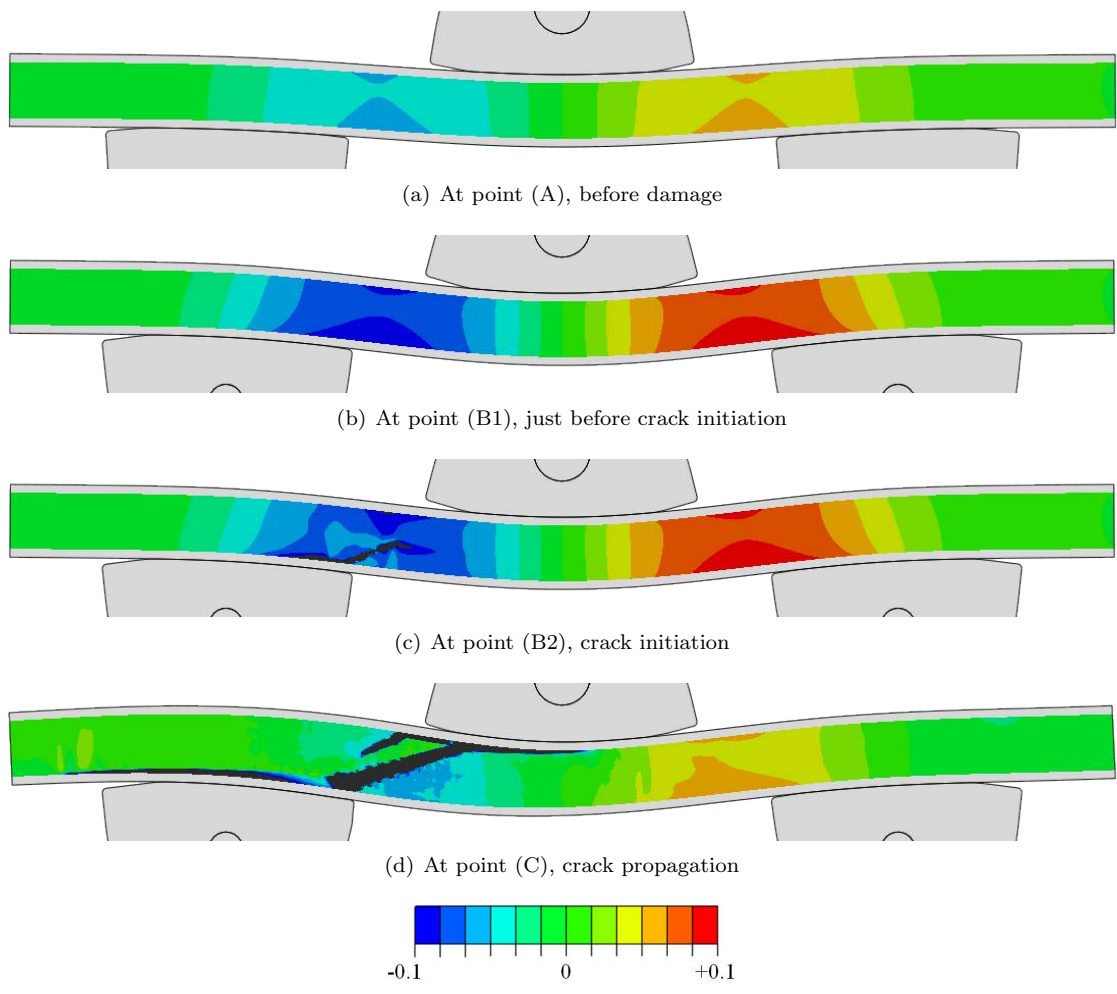


Figure 9. Transverse shear strain distribution from FEM simulation of quasi-static test. The colorbar is scaled to be feasible to compare with experiments. The black color shown is the out of colorbar range.

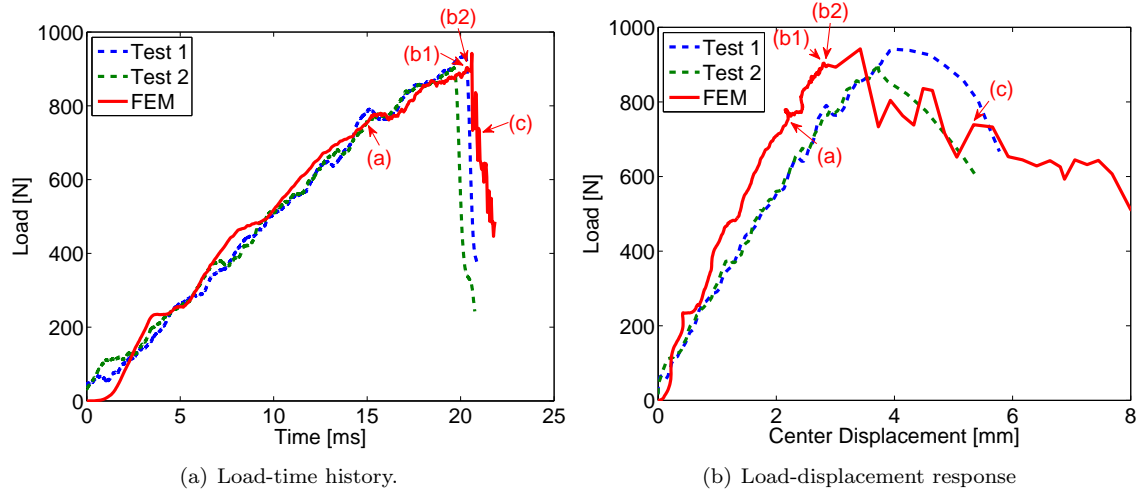


Figure 10. Comparisons of load history and load-displacement response between experiments and FEM simulation of 10J impact.

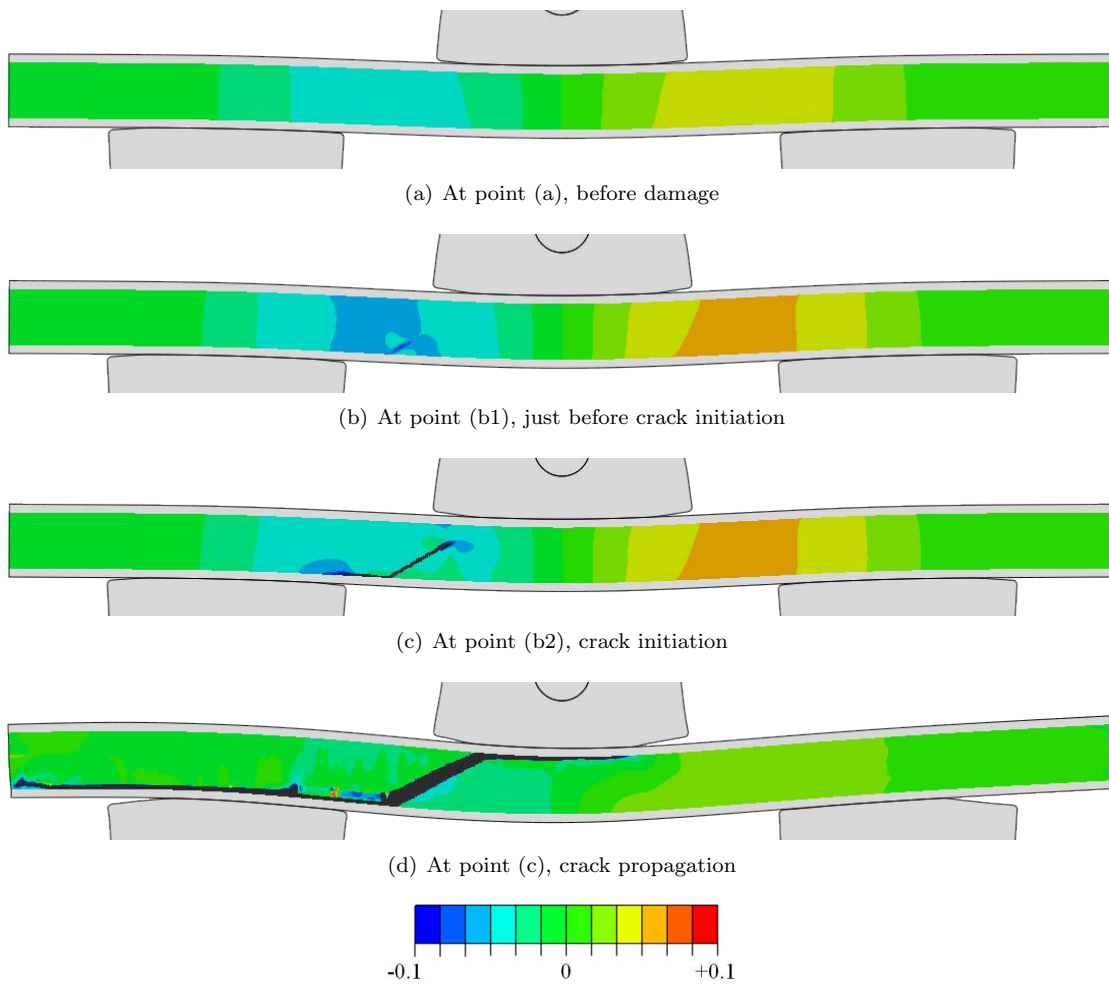


Figure 11. Transverse shear strain distribution from FEM simulation of 10J impact. The colorbar is scaled to be feasible to compare with experiments. The black color shown is the out of colorbar range.

displacement, which is the one commonly reported in literature. A new approach to measuring the displacement is considered to eliminate the large deformation influenced by the rubber pads. The center displacement is used to plot a secondary load-displacement response in Figure 8(b). The center displacement, defined in Figure 2, will provide more information on the flexural response of the sandwich structure, including material non-linearity. The FE model shows good agreement with experiments on the flexural response of the structure as well as capturing the peak load, and the location of failure initiation and propagation.

The low velocity impact simulations are compared against the experimental results, the load-time history as well as the load-displacement response are compared, as shown in Figure 10. The load-time history from the FE model agrees well with experimental results. The peak load predictions are in good agreement with experimental peak loads. From the load-displacement response, where the displacement is the center deflection of the structure (Figure 2), it can be seen that the experimental results are softer than the model predictions. The stiffness in the FE model is seen to be the same as that observed in the quasi-static experiments, and the reason for this change in stiffness needs further investigation.

The evolution of core failure and interface delamination for the quasi-static simulation is shown in Figure 9 and for the dynamic simulation in Figure 11, in terms of transverse shear strain, noting that the bound for the color contours is ± 0.1 so that it can be compared to the DIC results measured in experiments. The black color region in Figure 9 and 11 demonstrates that the absolute transverse shear strain is larger than 0.1. In the SCA, the secant modulus is degraded when the finite element reaches the critical stress and enters the post-peak strain softening zone, where the tangent stiffness is negative.⁷ In the progression of failure, the crack strain will replace the continuum strain as the dominant one. Therefore, the black color region can be considered as the crack. The failure initiation and propagation from the experiments was captured, the events are quite similar and will be described here after. The crack in the core initiates near the interface between the core and lower face-sheet with a 45° angle. It is worth noting that a small delamination occurs at the lower interface immediately after the small core crack initiates, starting from the core crack tip, which was also captured by the high-speed video in the impact experiments. Once the crack has been initiated it propagates through the core at a 45° angle as well as delaminations traveling rapidly to either side at a 135° angle, with respect to the core crack, resulting in a zig-zag shaped final failure of the structure. This zig-zag shaped failure, caused by the interaction of the matrix crack and the subsequent delamination is characteristic of the failure mode reported in many publications that deal with impact damage in composites.

IV. Conclusion

Experimental and numerical results for a sandwich composite beam under three point bending, both under quasi-static conditions as well as low velocity impact, have been presented. Detailed insight has been given into the failure mechanisms observed in the experiments, these details were captured in a 2D FE model by implementing failure with SCA. The FE model captures the flexural response of the static experiments as well as the onset of failure. The dynamic simulations show good agreement when it comes to load vs. time but the flexural stiffness is not captured correctly. The experimental results show rate softening which is not captured by the FE model. The reason for this softening could be due to micro cracking in the foam core almost instantaneously as the structure gets loaded, this would result in an over all stiffness softening rather than a progressive softening response. Further investigation is needed to prove this hypothesis.

Acknowledgments

The authors are grateful for the support and encouragement from Mostafa Rassaian, Salvatore Liguore and Steven Precup from the Boeing company.

References

- ¹Razi, H. and Kobayashi, A., "Delamination in cross-ply laminated composite subjected to low-velocity impact," *AIAA journal*, Vol. 31, No. 8, 1993, pp. 1498–1502.
- ²Zhang, X., Bianchi, F., and Liu, H., "Predicting low-velocity impact damage in composites by a quasi-static load model with cohesive interface elements," *Aeronautical Journal*, Vol. 116, No. 1186, 2012, pp. 1367–1381.
- ³Joshi, S. and Sun, C., "Impact induced fracture in a laminated composite," *Journal of Composite Materials*, Vol. 19, No. 1, 1985, pp. 51–66.

⁴Wang, J., Waas, A. M., and Wang, H., "Experimental and numerical study on the low-velocity impact behavior of foam-core sandwich panels," *Composite Structures*, Vol. 96, 2013, pp. 298–311.

⁵Heinrich, C. and Waas, A. M., "Investigation of progressive damage and fracture in laminated composites using the smeared crack approach," *Computers, Materials & Continua*, Vol. 35, No. 2, 2013.

⁶Rots, J., Nauta, P., Kuster, G., and Blaauwendraad, J., "Smeared crack approach and fracture localization in concrete," 1985.

⁷Zhang, D., Waas, A. M., and Yen, C.-F., "Progressive failure analysis on textile composites," *55th AIAA/ASME/ASCE/AHS/SC Structures, Structural Dynamics, and Materials Conference*, 2014.

⁸DMello, R. J. and Waas, A. M., "Inplane crush response and energy absorption of circular cell honeycomb filled with elastomer," *Composite Structures*, Vol. 106, 2013, pp. 491–501.